Separation Science and Technology
Publication details, including instructions for authors and subscription information:
http://www.informaworld.com/smpp/title~content=t713708471

Separation of *n*-Paraffins from Kerosene-Range Feedstock by Adsorption on Fixed-Bed Urea

Neguib M. Hassan[a]; Rasheed S. Al-Ameeri[b]; Fathi Oweysi[b]
[a] WESTINGHOUSE SAVANNAH RIVER TECHNOLOGY CENTER, AIKEN, SOUTH CAROLINA, USA
[b] CHEMICAL ENGINEERING DEPARTMENT, KUWAIT UNIVERSITY, SAFAT, KUWAIT

To cite this Article Hassan, Neguib M. , Al-Ameeri, Rasheed S. and Oweysi, Fathi(1994) 'Separation of *n*-Paraffins from Kerosene-Range Feedstock by Adsorption on Fixed-Bed Urea', Separation Science and Technology, 29: 3, 401 — 414
To link to this Article: DOI: 10.1080/01496399408002491
URL: http://dx.doi.org/10.1080/01496399408002491

SEPARATION SCIENCE AND TECHNOLOGY, **29**(3), pp. 401–414, 1994

Separation of *n*-Paraffins from Kerosene-Range Feedstock by Adsorption on Fixed-Bed Urea

---

NEGUIB M. HASSAN*
WESTINGHOUSE
SAVANNAH RIVER TECHNOLOGY CENTER
P.O. BOX 616, AIKEN, SOUTH CAROLINA, USA

RASHEED S. AL-AMEERI and FATHI OWEYSI
CHEMICAL ENGINEERING DEPARTMENT
KUWAIT UNIVERSITY
P.O. BOX 5969, SAFAT, KUWAIT

ABSTRACT

Experimental breakthrough curves have been obtained for *n*-paraffins from kerosene-range feedstocks on fixed-bed urea. The feedstocks used were unified heavy kerosene, straight-run kerosene, and naphtha–kerosene blend with initial *n*-paraffin contents of 29.31, 31.87, and 34.71 wt%, respectively. The breakthrough curves were measured in the temperature range 283–303 K and the feed flow rates 0.8–2.5 cm^3/min. The dynamic parameters for adsorption, such as the height of the mass transfer zone, the dynamic capacity, and the column efficiency, were determined from experimental breakthrough curves. The results from this study indicated that the *n*-paraffin molecules from unified heavy kerosene were more strongly adsorbed than those from straight-run kerosene or naphtha–kerosene blend, thereby revealing that *n*-paraffin adsorption on urea increased with the molecular length of the hydrocarbon. The values of the estimated apparent diffusion coefficients for *n*-paraffins from naphtha–kerosene blend ranged from 3.28×10^{-12} cm^2/s at 283 K to 5.06×10^{-12} cm^2/s at 303 K. The activated energy for diffusion was found to be 20.9 kcal/mol.

---

* To whom correspondence should be addressed.

INTRODUCTION

n-Paraffins have large and diverse industrial applications, such as the manufacture of biodegradable detergents, synthetic fatty acids, industrial surfactants, secondary alcohols, single cell proteins, lube oil additives, and various pharmaceutical products. *n*-Paraffins are separated from a wide range of petroleum feedstocks mainly by selective adsorption on molecular sieves and by urea adduction technique. The adsorption of *n*-paraffins on molecular sieves is largely characterized by the pore size and surface area of the adsorbent. Molecular sieves selectively adsorb molecules on the basis of size and shape, thereby adsorbing molecules of small diameter, such as *n*-paraffins, and excluding branched paraffins and aromatic hydrocarbons. The urea adduction method has been favorably employed in separating long-chain *n*-paraffins. However, a problem with the use of this method is that the adduct takes place in aqueous or alcoholic solution, making the method relatively complicated, usually unreliable, and often involves difficulty controlling the adduction rate (1). Nonnormal compounds, such as alkylbenzene, form adducts with urea, contributing to the impurities present in the separated *n*-paraffins from petroleum feedstocks (2).

The concept that a fixed bed of urea might be effective in separating *n*-paraffins from petroleum feedstocks has been examined by various investigators. For instance, McAdie and Frost (3) investigated the mechanisms for complex formation between *n*-octane vapor and solid urea. They measured the rate of the complex formation in the presence of water vapor. Matishev and Ben-Takhar (4) studied the dynamics of recovering *n*-nonane from mestilyene solution in a fixed bed of crystalline urea. They investigated the effects of bed height to diameter ratio and the feed flow rate on the concentration of *n*-nonane in the bed effluent at breakthrough. Makin et al. (5) investigated the performance of a semicontinuous fixed-bed urea to separate *n*-paraffins in the carbon range C_{10} to C_{20} from kerosene feedstocks. The bed was established by packing urea uniformly on a glass-fiber support and a continuous process of *n*-paraffin–urea association, washing, and dissociation was conducted. Makin et al. observed that urea crystals measured 20 μm in diameter after the first cycle and 90 μm after 20 cycles; each consisted of urea–*n*-paraffin association, washing, and dissociation. Kukanova et al. (6) employed a stationary bed of crystalline urea to recover both liquid *n*-paraffin with a low aromatic content and denormalized diesel fuel with a low pour point from high boiling petroleum fractions.

The adsorption of *n*-paraffins on urea is subject to the unusual properties of a urea–paraffin system. The *n*-paraffin triggers a structural transformation of urea from tetragonal crystals to hexagonal lattices. The lattices consist of six urea molecules each, forming hollow channels with critical diameters of about 5 Å. The volume of each lattice is about 650.66 $Å^3$ (7) compared to 776 $Å^3$ for molecular sieve type 5A (8). *n*-Paraffin molecules, which are characterized by minimum diameters of about 4.3 Å (9), can freely penetrate into both urea channels and molecular sieve cavities, and they are held inside by the same energetic interactions caused by van der Waals forces, London dispersion forces, and electrostatic attractions (10). The objective of this work was to measure the experimental breakthrough curves for the adsorption of *n*-paraffins on fixed-bed urea and to study the dynamic parameters, such as the dynamic capacity and the length of the mass transfer zone, that determine the efficiency of the adsorption process. The effects of temperature and feed flow rate on the dynamic parameters of the adsorption runs were studied. The apparent diffusion coefficients for *n*-paraffins and the activation energy for diffusion were also calculated.

EXPERIMENTAL SECTION

Materials

The petroleum feedstocks used in this study were supplied by Kuwait National Petroleum Co. and identified as unified heavy kerosene, straight-run kerosene, and naphtha–kerosene blend. These feedstocks were chosen because of their relatively high *n*-paraffin content. The physicochemical properties of the feedstocks are shown in Table 1. The distribution of *n*-paraffins in the feedstocks is shown in Table 2. The solvent used was isooctane (reagent grade) supplied by Matheson Co. with a stated purity greater than 99%. Crystalline urea was supplied by Hopkin and Williams Co., Chadwell Heath, Essex, England, and it had a density of 0.73 g/cm^3 and a moisture content of 0.2% by weight. The urea, obtained from Petrochemical Industries Co., Kuwait, was in pellet form and it also had a density of 0.73 g/cm^3. Prior to use, the urea was dried at 308–313 K and stored in a vacuum desiccator.

Procedure

A schematic diagram of the experimental apparatus for measuring adsorption breakthrough curves is shown in Fig. 1. The breakthrough measurements were carried out on two adsorption columns with two sizes of urea. The first column was made of a small glass tube, 15 mm i.d. × 700 mm long, equipped with a water jacket. It was charged with 100 g crystalline urea and it had a total bed height of 460 mm. The second column was

TABLE 1
Physicochemical Properties of Feedstocks

Property	Unified heavy kerosene	Straight-run kerosene	Naphtha–kerosene blend
Freezing point, °C	−12	−26	−53
Smoke point, mm	24	23	27
Specific gravity at 60°F	0.862	0.822	0.785
Refractive index at 20°C		1.4578	1.4380
Hydrogen content, wt%		13.63	14.06
Total *n*-paraffin, wt%	29.4	31.87	34.71
Naphthalenes, vol%		4.39	0.3
Olefins, vol%	0.0	0.0	0.0
Sulfur, wt%	0.52	0.67	0.14
Distillation:			
I.B.P. °C	241	204	164
10% recovery	262	228	175
50% recovery	279	249	187
90% recovery	304	74	201
E.P.	308	285	215

TABLE 2
Distribution of *n*-Paraffins in Kerosene-Range Feedstocks

n-Paraffin	Unified heavy kerosene	Straight-run kerosene	Naphtha–kerosene blend
C_8	—	0.48	0.92
C_9	—	0.77	3.71
C_{10}	—	1.54	10.56
C_{11}	—	2.00	9.15
C_{12}	0.40	2.82	6.43
C_{13}	3.20	4.54	3.73
C_{14}	6.65	6.18	0.21
C_{15}	5.75	5.87	—
C_{16}	5.40	3.98	—
C_{17}	4.85	2.34	—
C_{18}	2.25	1.20	—
C_{19}	0.60	0.15	—
C_{20}	0.15	—	—
C_{21}	0.06	—	—
Total, wt%	29.31	31.87	34.71

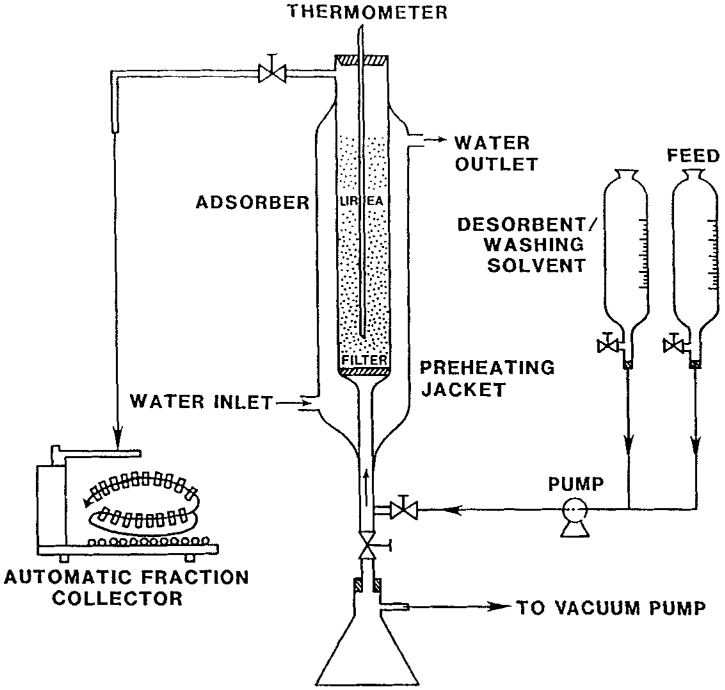

FIG. 1 Schematic diagram of the experimental apparatus for adsorption of n-paraffins on urea.

made of stainless steel tube (22.5 mm i.d. × 700 mm long) with a water jacket. This column was packed with 100 g urea pellets which had been crushed into particles of 1–2 mm size. The total bed height of the urea was 270 mm. Special care was taken when packing the columns to ensure that the same amount of urea was used per unit length. In each run the feedstock was thoroughly blended with 10% by volume of methanol activator in a reservoir, and the mixture was continuously stirred to ensure a uniform influent concentration at the inlet to the column. The purpose of using the activator was to free the surface of tetragonal urea crystals and to aid in the formation of a hexagonal lattice, therefore allowing the diffusion of n-paraffin molecules. The columns were maintained at the desired temperatures by circulating water from a constant temperature bath through the water jackets. The column temperatures were measured with thermocouples mounted in the center of the bed. The feedstock was fed to each column from the bottom at a constant flow rate. The effluent samples were collected at equal time intervals from the top of the columns by means of an automatic sample collector. The adsorption run was continued until the bed was exhausted, as indicated by the refractive index (RI) reading of the effluent samples when compared to that of the original feedstock.

After the adsorption phase was completed, each column was drained before washing and the feed entrained in the bed was removed from the bottom of the column. The bed was washed with the isooctane solvent by pumping it through the bottom of the column at a flow rate twice as high as that of the adsorption phase. The washing phase was terminated when the refractive index reading of the effluent stream was about the same as that of the solvent. Upon completion of the washing phase, the column temperature was raised to 353 K and isooctane was fed to the column from the bottom at a low flow rate. The effluent stream containing *n*-paraffin in isooctane was collected from the top of the column. The desorption phase was continued until the refractive index reading of the effluent stream was equal to that of the solvent. The *n*-paraffin was later separated from the solvent by distillation.

Analysis

Analysis of the original feed and the effluent samples from the columns was performed with a gas chromatograph, Hewlett-Packard model 5840A, equipped with a single flame ionization detector and an electronic integrator. A stainless steel column 2 m long × 3.2 mm diameter, packed with 10% OV-101 methyl silicone fluid on a Chromasorb W-HP 100/120 Hewlett-Packard packing, was used for this purpose. A standard sample consisting of C_{12}–C_{21} carbon atoms was prepared and used to calibrate the GC system. The total *n*-paraffin content in the effluent samples was determined using an area analysis of the peak size of each component produced from the gas chromatograph. For each sample, three analyses were performed to obtain the mean value. The average absolute deviation from the mean was estimated to be 0.5 wt%.

Theory

Expressions relating dynamic parameters for adsorption to experimental breakthrough curves have been developed by Michael (11). For instance, the height of the mass transfer zone, in which adsorption takes place, was given by

$$h_z = L_0 \left[\frac{(t_e - t_b)}{t_e - (1 - F)(t_e - t_b)} \right] \tag{1}$$

where L_0 is the total bed height, t_b is the breakthrough time, t_e is the bed exhaustion time, and F is the fraction of the bed in the mass transfer zone that is still capable of use. The parameter h_z was related to the efficiency of the column in the mass transfer zone or the percent saturation of the bed according to the equation

$$\gamma = \frac{(L_0 - Fh_z)100}{L_0} \tag{2}$$

The dynamic capacity of the adsorbent was determined from experimental breakthrough curves up to the point of bed exhaustion according to the equation

$$q_m = \frac{Q\rho}{m}\int_{t_b}^{t_e}\left(1 - \frac{C}{C_0}\right)dt \tag{3}$$

where Q is the feed flow rate, ρ is the density of the feed, C_0 is the initial concentration of the adsorbate in the feed, C is the concentration in the effluent sample at time t, and m is the mass of the adsorbent. The integral in Eq. (3) represents the total area behind the breakthrough curve. The performance of the adsorption column was evaluated in terms of the dynamic parameters in such a way as to minimize the height of the mass transfer zone and to maximize the dynamic capacity.

RESULTS AND DISCUSSION

Experimental breakthrough curves for *n*-paraffins on crystalline urea were obtained at 295 K. Replicate runs were made to check the reproducibility of the breakthrough measurements. A plot of two sets of data obtained at 295 K is shown in Fig. 2. It can be seen that the adsorption of *n*-paraffins on urea can be measured reproducibly with an average error of less than 7%. The experimental breakthrough curves for *n*-paraffins from different types of feed on urea pellets are shown in Fig. 3. It is important to note that the feedstocks used had different compositions. For instance, naphtha–kerosene blend had an initial *n*-paraffin content of 34.71 wt% with carbon atoms in the C_8–C_{14} range whereas straight-run kerosene feed had a total *n*-paraffin content of 31.87 wt% with carbon atoms in the C_8–C_{19} range. The unified heavy kerosene (29.31 wt%) contained heavier *n*-paraffins in the C_{12}–C_{21} carbon range. The dynamic parameters obtained for *n*-paraffins adsorbed from different feedstocks are summarized in Table 3. The height of the mass transfer zone (h_z) during adsorption decreased in the following order: naphtha–kerosene blend >

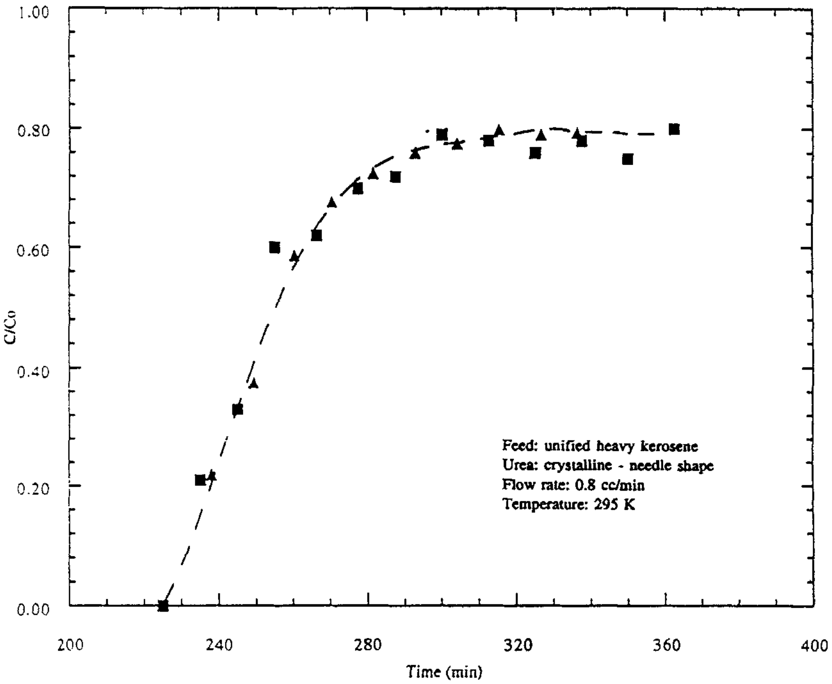

FIG. 2 Reproducibility of the experimental breakthrough curves.

straight-run kerosene > unified heavy kerosene. The dynamic capacity of urea for *n*-paraffins adsorbed from unified heavy kerosene was 17.3 g/100 g urea as compared to that adsorbed from straight-run kerosene (16.2 g/100 g urea) or naphtha–kerosene blend (11.5 g/100 g urea). This result shows the significance of the interactions between CH_2 groups in the *n*-

TABLE 3
Dynamic Parameters for Adsorption of *n*-Paraffins from Kerosene-Range Feedstocks on Urea

Feedstocks	h_z,[a] mm	γ, %	q_m, g/100 g of urea
Unified heavy kerosene	49.7	93	17.3
Straight-run kerosene	69.5	95.4	16.2
Naphtha–kerosene blend	70.4	92.7	11.5

[a] Based on a total bed height of 270 mm.

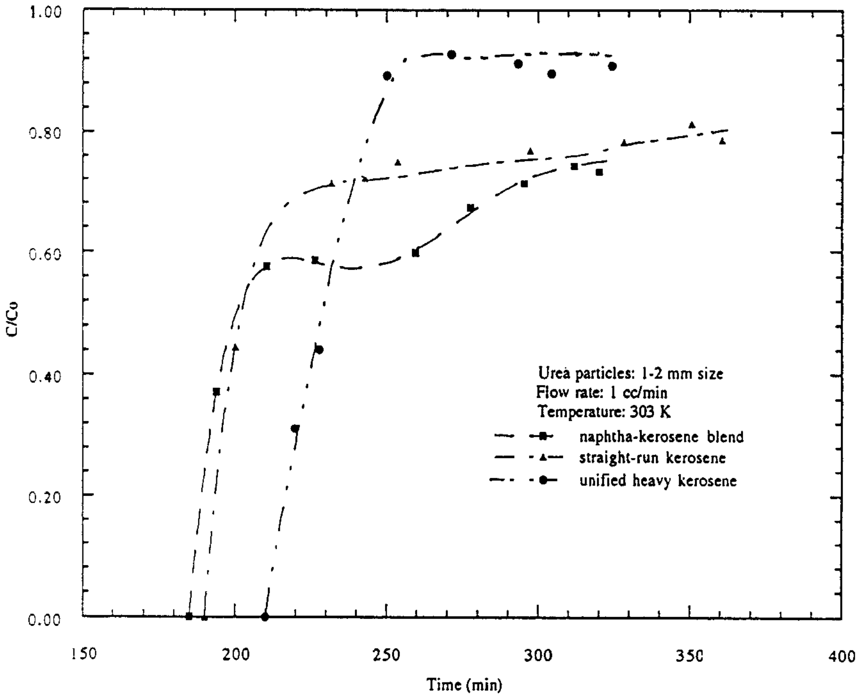

FIG. 3 Experimental breakthrough curves for *n*-paraffins from kerosene-range feedstocks on urea.

paraffin chain and the urea lattice. Since the lengths of the *n*-paraffin molecules increases on going from naphtha–kerosene blend to unified heavy kerosene, the interactions of *n*-paraffin molecules with the urea lattice increase. Thus, high molecular weight *n*-paraffins in unified heavy kerosene feed were more strongly adsorbed by urea than low molecular weight *n*-paraffins in either straight-run kerosene or naphtha–kerosene blend, as expected.

The number of adsorbed molecules per unit cell was calculated according to the equation

$$M_u = q_m N / n \tag{4}$$

where M_u is the number of molecules per unit cell, q_m is the saturation adsorption capacity in mol/g, N is Avogadro's number (6.023×10^{23} molecules/mol), and n is the number of unit cells/g urea (2.105×10^{21}). The number of adsorbed molecules per unit cell was constant for all three feedstocks (approximately 0.22 molecules/unit cell). This result suggests that the *n*-paraffins from all three feedstocks have the same difficulty in diffusing through the urea channels. Therefore, the interactions of the molecules with the urea lattice were caused by the molecular length, which increased per additional CH_2 group in the *n*-paraffin chain. The number of molecules per unit cell obtained in this study is one order of magnitude less than the values obtained in a previous study (12) for adsorption of C_{12}–C_{16} individual *n*-alkanes from isooctane solution on crystalline urea in a batch system.

The change in adsorption characteristics with temperature was investigated by measuring the experimental breakthrough curves for *n*-paraffins on urea at 283, 295, and 303 K. As shown in Fig. 4, the shape of the breakthrough curves became steeper as the temperature was increased and the *n*-paraffin broke through the column at a faster rate. The dynamic parameters, which are presented in Table 4, illustrate the overall temperature effect. The dynamic capacity of urea for *n*-paraffins decreased from 19.6 g/100 g urea at 283 to 12.5 g/100 g urea at 303 K. The height of the

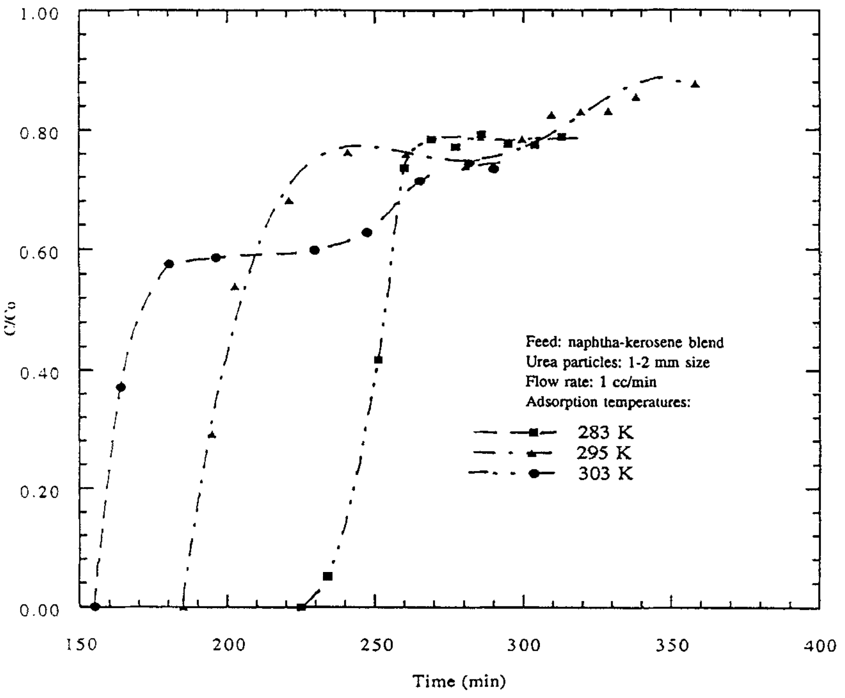

FIG. 4 The effects of temperature on the adsorption of *n*-paraffins on urea.

TABLE 4
Temperature Effects on the Dynamic Parameters for Adsorption of *n*-Paraffins[a] on Urea

Temperature, K	h_z,[b] mm	γ, %	q_m, g/100 g of urea
283	30.1	92.6	19.6
295	49.2	93.6	13.4
303	60.1	94.1	12.5

[a] From naphtha–kerosene blend.
[b] Based on a total bed height of 270 mm.

mass transfer zone (h_z) during adsorption increased from approximately 30 mm at 283 K to 60 mm at 303 K. The increase in temperature has a tendency to weaken the highly energetic interactions between the methyl group in the *n*-paraffin chain and the oxygen atoms of the urea lattice walls, resulting in a lower dynamic capacity and a higher mass transfer zone. Although the temperature effect is evident, the column efficiency still remained very high (>92%) in this low temperature range. The scatter in the experimental adsorption data at breakthrough clearly revealed that the effects of the heat of adsorption existed in the column despite the effort to maintain the column at an isothermal condition.

Figure 5 shows the experimental breakthrough curves for *n*-paraffin on urea measured at flow rates ranging from 0.8 to 2.5 cm^3/min. The experimental results show that the flow rate had a definite effect on the shape of the breakthrough curves. The breakthrough curves became steeper as the flow rate was increased and the breakthrough time was shorter. Since the mechanism of *n*-paraffin adsorption on urea is diffusion controlled, the rate of diffusion of *n*-paraffin molecules into the urea channels increased as the feed flow rate was decreased. As a result, the amount of *n*-paraffin adsorbed at low flow rates became higher than those adsorbed at relatively higher flow rates. This result is clearly illustrated in Table 5. The dynamic capacity of urea for *n*-paraffins from unified heavy kerosene was 19.3, 9.2, and 6.7 g/100 g urea at feed flow rates of 0.8, 2, and 2.5 cm^3/min, respectively. Based on a total bed height of 460 mm, the height of h_z increased from about 247 mm at 0.8 cm^3/min to 431 mm at 2.5 cm^3/min. The effective efficiency of the adsorption column (γ) dropped from about 88% to less than 70% in this range of feed flow rate. It was found that when the feed flow rate was above 2.5 cm^3/min, a region of stable adduct formed at the bottom of the column and the bed became sticky (this was observed visually), thereby increasing the hydraulic resistance to the flow of the feed.

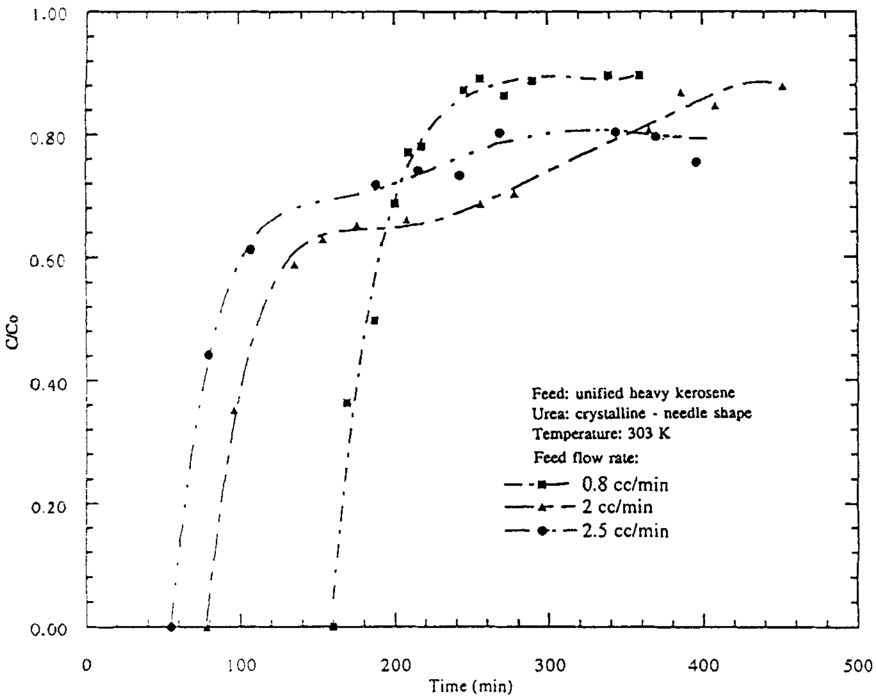

FIG. 5 The effects of feed flow rate on the adsorption of *n*paraffin on urea.

TABLE 5
The Effect of Feed Flow Rate on the Dynamic Parameters for Adsorption of *n*-Paraffins[a] on Urea

Flow rate, cm^3/min	h_z,[b] mm	γ, %	q_m, g/100 g of urea
0.8	247	88.2	19.3
2	423	75.9	9.2
2.5	431	69.8	6.7

[a] From unified heavy kerosene.

[b] Based on a total bed height of 460 mm.

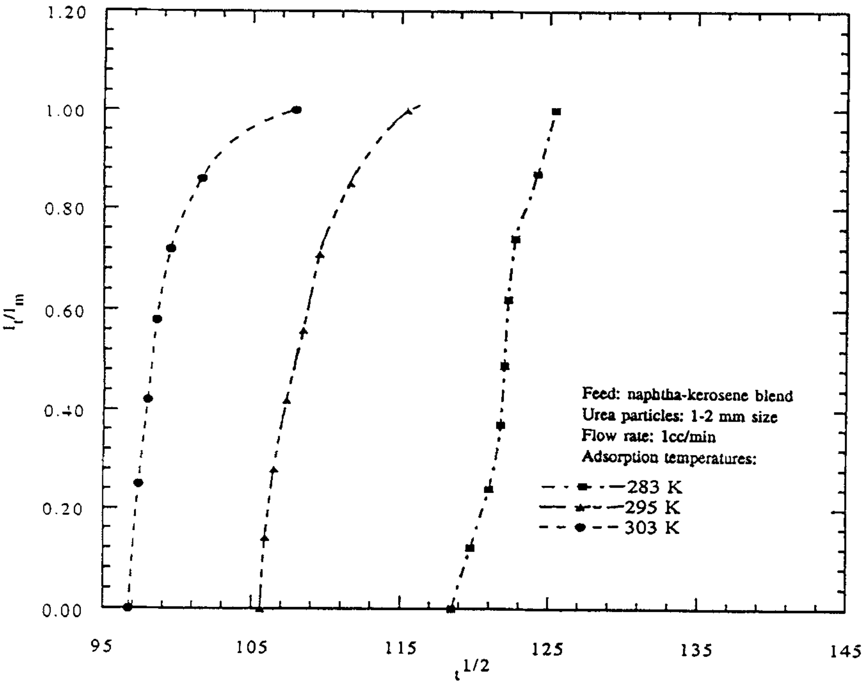

FIG. 6 A typical plot of the fractional uptake curves vs $t^{1/2}$.

The apparent diffusion coefficients of *n*-paraffin molecules into urea channels were determined from an analysis of the experimental breakthrough curves at 283, 295, and 303 K. The fractional uptake was plotted vs $t^{1/2}$ according to the equation

$$\frac{q_t}{q_m} = 2\left(\frac{A}{V}\right)\sqrt{\left(\frac{D_a t}{\pi}\right)} \tag{5}$$

where q_t and q_m are the amounts of *n*-paraffin molecules adsorbed at time t and at bed exhaustion, A is the lattice surface area, V is the lattice volume, and D_a is the apparent diffusion coefficient. A typical plot of the fractional uptake, q_t/q_m, vs $t^{1/2}$ is shown in Fig. 6. The apparent diffusion coefficients obtained from the slope of the initial portions of the uptake curves in Fig. 6 were found to be 3.28×10^{-12}, 5.06×10^{-12}, and 5.06×10^{-12} cm^2/s at 283, 295, and 303 K, respectively. These values are in close agreement with the value reported by Calderbank and Nikolov for the diffusion of normal hydrocarbons into solid urea (13).

The activation energy for diffusion was calculated according to the equation

$$D_a = D_0 \exp(-E/RT) \tag{6}$$

where E is the activation energy, D_0 is a preexponential constant, T is the temperature, and R is the universal gas constant. The activation energy thus obtained for short-time diffusion coefficients is about 20.9 kcal/mol. The calculated activation energy would represent the energy barrier for the *n*-paraffin molecules entering the urea channels.

ACKNOWLEDGMENT

This work was partly supported by Grant EC 027 from the Research Council of Kuwait.

REFERENCES

1. W. F. Avery, U.S. Patent 3 422 005 (1969).
2. R. S. Al-Ameeri and F. A. Oweysi, *Ind. Eng. Chem., Prod. Dev., 23*(4), 637 (1984).
3. H. G. McAdie and G. B. Frost, *Can. J. Chem., 36*, 635 (1958).
4. V. A. Matishev and N. Ben-Takhar, *Chem. Technol. Fuels Oil, 15*(5), 303 (1981).
5. E. C. Makin, C. H. Glass, C. H. Middlebrooks, and J. M. Farrar, *Ind. Eng. Chem., Process Des. Dev., 3*(3), 226.
6. K. P. Kukanova, A. G. Sardanashvili, and V. A. Matishev, translated from *Khim. Tekhnol. Topl. Masel, 7*, 18 (1972).
7. A. E. Smith, *Acta Cryst., 5*, 224 (1952).
8. J. Xiao and J. Wei, *Chem. Eng. Sci., 47*(5), 1143 (1992).
9. D. W. Breck, *Zeolite Molecular Sieves*, Wiley, New York, 1974, p. 636.
10. W. Schirmer, G. Friedrich, A. Grossman, and H. Stach, *Proceedings of the First International Conference on Molecular Sieves*, London, 1967, p. 285.
11. A. S. Michael, *Ind. Eng. Chem., 44*(8), 1922 (1952).
12. R. S. Al-Ameeri, F. Owesi, and N. M. Hassan, *Ind. Eng. Chem. Res., 30*(1), 202 (1990).
13. P. H. Calderbank and N. S. Nikolov, *J. Phys. Chem., 60*, 1 (1956).

Received by editor March 15, 1993